Friction in mid-latitude cyclones: an Ekman-PV mechanism

Article

Accepted Version

Friction in mid-latitude cyclones: an Ekman-PV mechanism

I. A. Boutle[a*], S. E. Belcher[ab] and R. S. Plant[b]

[a]Met Office, Exeter, UK

[b]Department of Meteorology, University of Reading, UK

Atmospheric Science Letters

March 17, 2014

Abstract

The mechanism by which the atmospheric boundary layer reduces the intensity of mid-latitude cyclones is investigated. It is demonstrated that two alternative theories, Ekman pumping and the baroclinic potential vorticity (PV) mechanism, in fact act in union to maximise the spin-down. Ekman pumping aids the ventilation of PV from the boundary layer, and shapes the resulting PV anomaly into one of increased static stability. PV inversion techniques are used to demonstrate how this anomaly reduces the coupling between the upper- and lower-levels within the cyclone, reducing the growth rate.

1 Introduction

The presence of friction in the atmospheric boundary layer is known to reduce the intensity of mid-latitude cyclones (Anthes and Keyser, 1979; Valdes and Hoskins, 1988; Boutle *et al.*, 2010). The reduction on any metric of intensity is typically $\approx$ 40% from the inviscid solution. However, the mechanism by which this reduction is achieved is still a topic of active discussion. Traditionally, the barotropic Ekman pumping mechanism is assumed to be the dominant process. Surface stress causes wind-turning in the boundary layer, forcing convergence of near surface winds towards the low centre. This convergence creates ascent at the boundary layer top due to continuity. The ascent squashes the interior vortex within the cyclone. Beare (2007) has demonstrated that Ekman pumping is still a good method for interpreting the cyclone response to boundary layer forcing, especially in systems with strong low-level jets.

Mid-latitude cyclones are inherently baroclinic in nature, and therefore potential vorticity (PV) is the natural variable to describe their evolution. Adamson *et al.* (2006) and Plant and

*Correspondence to: Ian Boutle, Met Office, FitzRoy Road, Exeter, EX1 3PB, UK. E-mail: ian.boutle@metoffice.gov.uk

Belcher (2007) describe the baroclinic PV mechanism, whereby PV generated in the boundary layer (due to a component of stress anti-parallel to the tropospheric thermal wind) is advected along the warm-conveyor belt. This ventilates it from the boundary layer, where it turns cyclonically and accumulates as a positive PV anomaly above the low pressure centre. The presence of this PV anomaly increases the static stability of the free troposphere, acting as an insulator to reduce the coupling between the upper- and lower-levels of the cyclone. This leads to a reduction in the cyclone growth rate.

The papers of Adamson *et al.* (2006) and Beare (2007) appear contradictory, each providing evidence for two, seemingly independent, mechanisms. Boutle *et al.* (2007) shed some light on the differences between the studies, demonstrating that both mechanisms were present in a single simulation. But they did not attempt to reconcile the relative importance of each mechanism, and this is the aim of the present paper. Through an analysis of the Eady model in Section 2 and idealised numerical simulations in Section 3, we will demonstrate that the two mechanisms cannot be considered independently, but rather they both form a crucial component of the spin-down mechanism.

2 Eady model analysis

The Eady (1949) model is a simple yet effective mathematical model to describe baroclinic instability. It is based on the assumption that Quasi-Geostrophic Potential Vorticity is conserved, i.e.

$$\frac{\partial^2 \psi_g}{\partial x^2} + \frac{\partial^2 \psi_g}{\partial y^2} + \frac{f^2}{N^2}\frac{\partial^2 \psi_g}{\partial z^2} \equiv 0, \tag{1}$$

where ψ_g is the geostrophic streamfunction, f is the Coriolis parameter and N^2 is the (assumed constant) static stability. Boundary conditions are applied at the boundary-layer top and tropopause by the linearised thermodynamic equation:

$$f\frac{\partial^2 \psi_g}{\partial t \partial z} + uf\frac{\partial^2 \psi_g}{\partial x \partial z} + \frac{g}{\theta_0}\frac{\partial \theta}{\partial y}\frac{\partial \psi_g}{\partial x} = -N^2 w, \tag{2}$$

where u, w and θ are the horizontal and vertical wind-speeds, and potential temperature, at the boundaries, g is the gravitational acceleration and θ_0 is a reference potential temperature. Typically $w = 0$ on the boundaries is assumed and normal mode solutions to Eq. 1 with appropriate scaling parameters allow calculation of the cyclone growth rate as a function of zonal wavenumber. This is shown graphically in Figure 1, and mathematical details can found in Pedlosky (1979) or Boutle (2009).

To consider the effect of Ekman pumping in the boundary layer, we can instead allow w at the bottom boundary only to be given by

$$w = \sqrt{\frac{K_m}{2f}}\left(\frac{\partial^2 \psi_g}{\partial x^2} + \frac{\partial^2 \psi_g}{\partial y^2}\right), \tag{3}$$

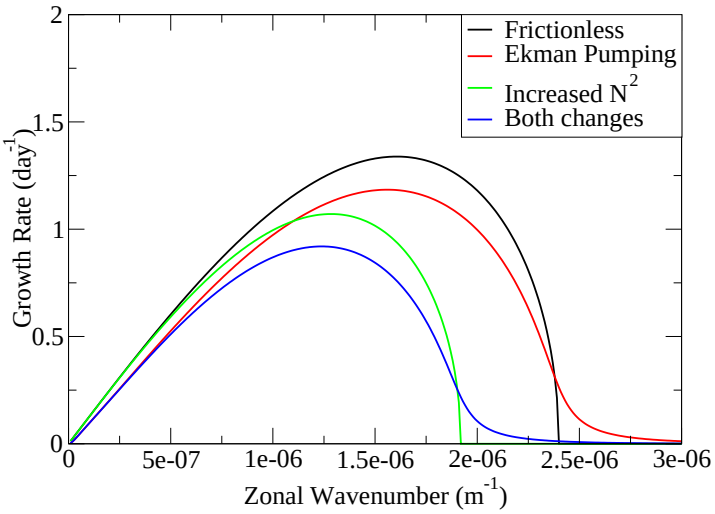

Figure 1: Growth rate curves for the frictionless Eady model (black), Eady model with Ekman pumping (red), Eady model with 25% increased Static Stability (green) and Eady model with both changes (blue).

as derived from Ekman theory, where K_m is the eddy diffusivity for momentum within the boundary layer. Taking $K_m = 10$ m^{2}s^{-1}, which is representative of what is observed in the numerical simulations of Section 3, the Ekman pumping solution is achieved. This shows a modest reduction of 12% in the peak growth rate.

To consider the effect of the baroclinic PV mechanism, we can impose an increase in N^2 consistent with the effect of the PV anomaly. For simplicity, we represent this as a 25% increase throughout the depth of the troposphere, again representative of what is observed in the numerical simulations of Section 3. This shows a larger reduction in the peak growth rate (20%), but also causes a shift of the peak towards lower wavenumbers (larger cyclones). This means that in idealised simulations, such as those of Adamson *et al.* (2006), where the wavenumber is fixed, the reduction in growth rate would be larger (30% for their case of wavenumber 6). When both mechanisms are included, the largest reduction in growth rates is achieved (32% at the peak; 42% at wavenumber 6), which is much closer to the observed reduction in growth rates. Therefore, this simple Eady model analysis suggests that both mechanisms are necessary for a reduction in growth rate similar to reality. But how do they interact in a real cyclone?

3 Idealised cyclone simulations

Boutle *et al.* (2007) present several idealised cyclone simulations, and in this section we investigate further their experiment which showed both of the possible spin-down mechanisms at work. This was created by adding a meridional sea-surface temperature gradient (similar to Adamson *et al.*, 2006) to the control experiment of Beare (2007). The simulations take a

dry atmosphere, in which an idealised jet structure in thermal wind balance with a temperature profile is perturbed by the addition of an upper-level vortex, triggering cyclogenesis. The simulation shows similarity to the conceptual model of Shapiro and Keyser (1990), and full details of the set-up can be found in Beare (2007) and Boutle (2009).

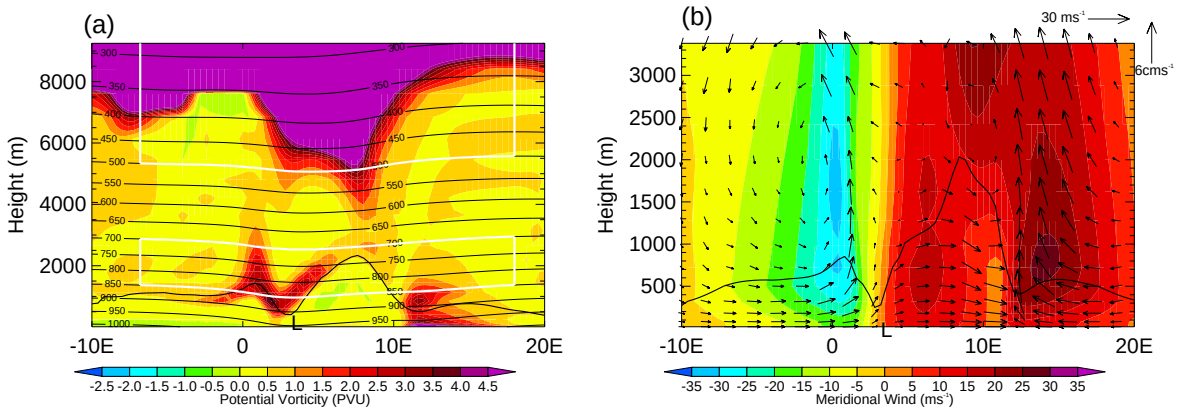

Figure 2: East-west cross-section through the low centre after 48 hours, showing (a) potential vorticity (coloured) and pressure (contoured), and (b) (u, w) wind vectors and v-wind (coloured). The solid black line represents the boundary-layer top and the white boxes in (a) outline the regions in which PV was defined as being anomalous.

Figure 2 shows cross-sections of the PV and vertical velocity through the low centre. Behind the low centre, the wind structure appears similar to what we would expect from Ekman theory: convergence towards the low centre, ascent into the free troposphere and a return flow completing the circulation. However, ahead of the low centre, this pattern is not obvious. Instead, the low level winds are converging at the cold front, strengthening the front and causing ascent ahead of it. This ascent assists with the low level ascent of the warm-conveyor belt, and gives the first suggestion that the two mechanisms may be connected. The low level ascent of the warm-conveyor belt, driven by Ekman convergence in the boundary layer, is responsible for the ventilation of the baroclinically generated PV into the free troposphere. Secondly, as the PV accumulates above the low centre, it is accumulating in the region of ascent generated by Ekman convergence. This ascent lifts isentropes in the region of the PV anomaly, squashing them together and shaping the PV anomaly into one of increased static stability.

To investigate the effect this low level PV anomaly has on the coupling between the upper- and lower-levels of the cyclone, we have conducted a PV inversion. We follow the technique of piecewise PV inversion (Davis and Emanuel, 1991; Stoelinga, 1996), defining the anomaly of interest within the domain and calculating its effect on the circulation. The inversion technique and code is discussed in Ziemianski (1994) and Ahmadi-Givi *et al.* (2004), and works by completing two PV inversions. A sub-domain is defined, which contains the PV anomaly of interest, and in the first inversion the complete PV field within this sub-domain is inverted

to obtain the streamfunction and geopotential height fields. Boundary conditions for the full domain are given by the potential temperature. The second inversion removes the PV anomaly by setting the PV to a background value and the modified PV field is then inverted again. The flow induced by the anomaly is determined as the difference between the two inversion results.

Figure 2a shows a PV cross-section through the low pressure centre at the time when the inversion was conducted. The balance condition is only applicable to frictionless flow, and therefore the boundary layer must be removed from the inversion domain. The inversion code works on pressure levels, so the boundary-layer top was defined as the 900 hPa surface and represents the bottom boundary of the inversion domain. Figure 2a shows that a more complex definition of the boundary-layer top (based on the bulk Richardson number, see Sinclair *et al.*, 2010, for example) is very close to the 900 hPa surface across much of the cyclone. Only behind the cold front (between the low centre and 10E) does the boundary-layer top deviate greatly from the 900 hPa surface, here extending up to 750 hPa. However, if 750 hPa were to be used at the boundary-layer top definition, then most of the baroclinically-generated PV anomaly would also be excluded from the inversion domain.

The first inversion concerned the PV anomaly sitting above the boundary-layer top above the cyclone centre. The PV anomaly was defined to exist between 850 and 700 hPa, and the lower white box shown in Figure 2a illustrates the sub-domain containing the anomalous PV. The background value used was obtained from a simulation with no boundary-layer scheme operating. This definition captures the bulk of the baroclinically-generated PV anomaly, whilst excluding any other PV structures. Consistent with the results of Beare (2007), the inversion demonstrates that the low-level PV anomaly has a positive static stability anomaly and small cyclonic circulation associated with it. The positive vorticity anomaly is modest, with an increase in vorticity of $\approx 30\%$ being induced by the PV anomaly. Consistent with the arguments Adamson *et al.* (2006), the PV anomaly is predominantly associated with stability, with a doubling (i.e. a 100% increase) in the static stability being induced by the anomaly. Such a strong increase in static stability will act to reduce the cyclone growth rate.

The instantaneous effect of the positive PV anomaly is to generate a cyclonic circulation, but the time-integrated effect of the increased static stability should cause spin down by reducing the coupling between tropopause and surface levels within the cyclone. Therefore, two further PV inversions were carried out in an attempt to ascertain the shielding influence of this low-level PV anomaly.

The cyclone grows due to the interaction of the upper-level (tropopause) PV anomaly with the surface potential temperature distribution. The positive vorticity associated with the upper-level anomaly enhances the surface temperature wave, causing the cyclone to intensify. Therefore, a PV inversion on this upper-level anomaly will show its effects at the surface. If the baroclinic PV mechanism is acting as expected, the influence of this upper-level anomaly

at the surface should be greater if the lower-level anomaly is not present; i.e. if there is no shielding effect.

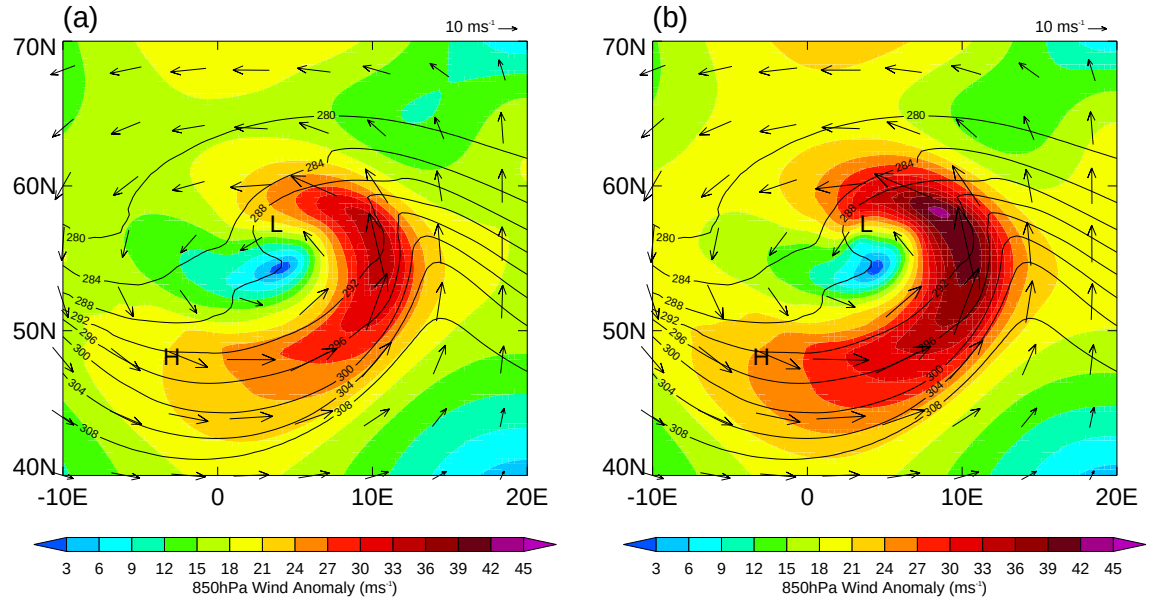

Figure 3: PV inversion results at 48 hours showing the flow induced by the upper-level (tropopause) PV anomaly at 850 hPa (colours and vectors) (a) with the low-level PV anomaly present and (b) without the low-level PV anomaly present. Also plotted are contours of potential temperature at 900 hPa.

An upper-level anomaly was defined as the difference between the full PV field and the time-mean PV field over the cyclone life-cycle. The upper-level sub-domain for anomalous PV was between 500 and 200 hPa in the vertical, and the upper white box in Figure 2a demonstrates that this definition does indeed capture the trough. Figure 3a shows the 850 hPa winds induced by the upper-level PV anomaly with the low-level anomaly present. It is clear that the winds are acting to enhance the wavelike pattern shown in the 900 hPa potential temperature. Figure 3b shows the same diagnostics when the low-level baroclinically-generated PV anomaly (lower white box in Fig. 2a) is removed. With the low-level anomaly removed, the influence of the upper-level feature is enhanced. This shows that without the low-level anomaly present, the upper-level feature would have a greater influence on the surface potential temperature field, eventually leading to a stronger cyclone forming.

So far we have presented results which suggest that, rather than being two competing mechanisms for cyclone spin-down, there is some constructive interaction between Ekman pumping and the baroclinic PV mechanisms. Beare (2007) conducted two sensitivity experiments that involved switching off the boundary-layer parametrization in either stable or unstable boundary layers. This was achieved by determining at each timestep whether the boundary layer was stable or unstable, given by the sign of the surface buoyancy flux. The effect of boundary

layer turbulence was then removed by setting all eddy diffusivity parameters (e.g. K_m) to zero for the relevant boundary layer type. Here, we also conduct a NO-BL experiment, in which the boundary-layer parametrization is not included. Whilst it was observed by Beare (2007) that the case with only the stable boundary layer active had a greater affect on cyclone intensity, the reasons for this were not fully investigated. In our simulation, the differences between the case with only an active stable boundary layer (NO-CBL) and the case with only an active convective boundary layer (NO-SBL) are much smaller; indeed, both changes have similar size effects on the cyclone intensity (Figure 4a).

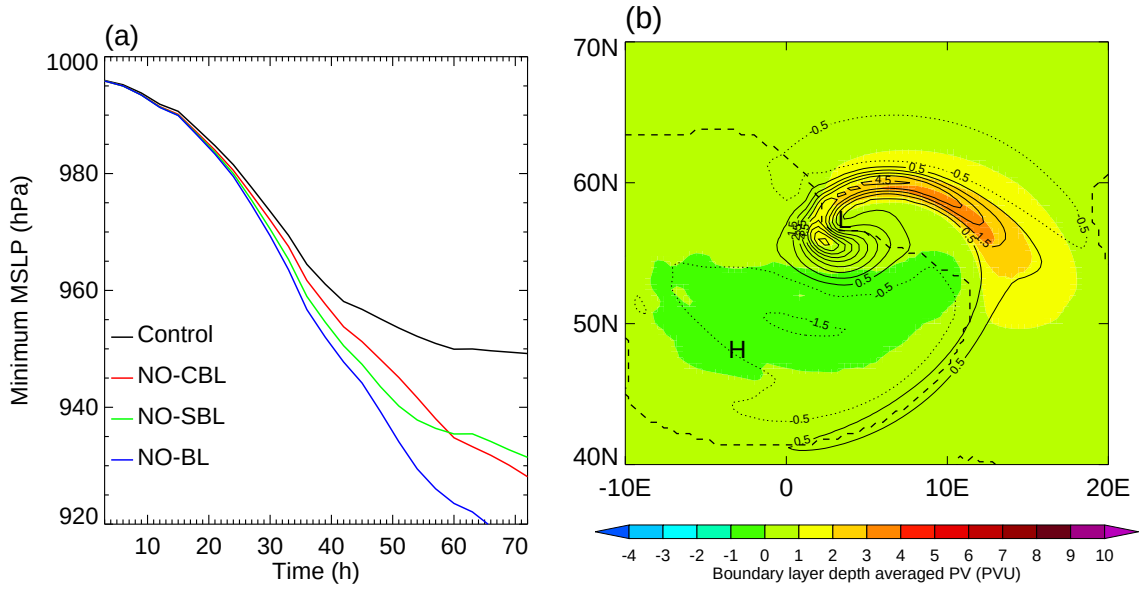

Figure 4: (a) Time evolution of minimum sea-level pressure for the control simulation (black), NO-CBL (red), NO-SBL (green) and NO-BL simulation (blue). (b) Control simulation at 48 hours showing boundary-layer depth-averaged PV (coloured), Ekman pumping velocity (black contours for positive values and dotted for negative values) and the demarcation between stable and unstable boundary layers (dashed line).

Figure 4b shows the Ekman pumping velocity and boundary-layer depth-averaged PV in the control simulation, along with the line separating stable and unstable boundary layers. It is noticeable that most of the boundary-layer PV (and the PV generation; not shown) is located within the stable boundary layer. Therefore, simulation NO-SBL represents effectively a no-PV mechanism simulation. The Ekman pumping is more complicated as it is spread across the stable and unstable boundary layers. However, the strongest Ekman pumping, located coincident with the cyclone centre, is in the convective boundary layer. This is the Ekman pumping that should be most effective at producing vortex squashing in the interior, since this is the also location of highest vorticity. Hence, simulation NO-CBL should remove this effect, leaving only weak Ekman pumping in the warm-conveyor belt region, which as mentioned previously, is needed to ventilate the frictionally–generated PV.

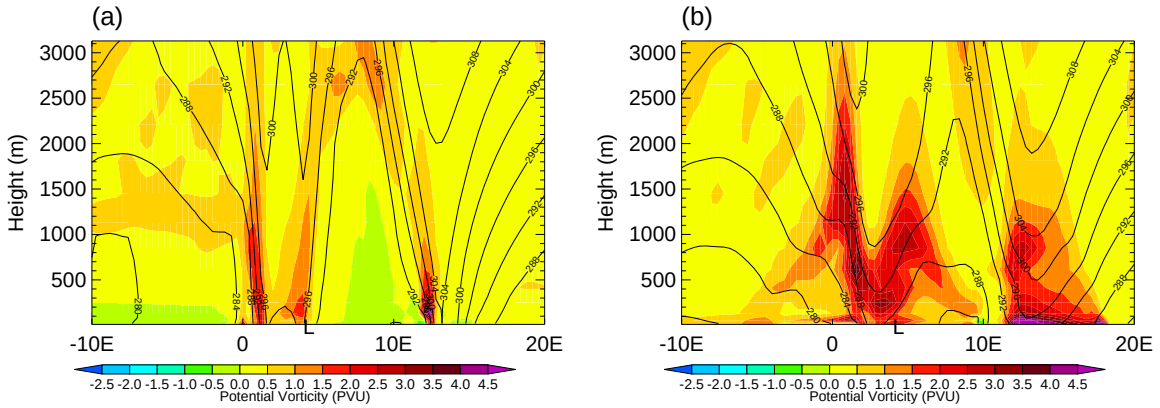

Figure 5: East-west cross-section through the low centre at 48 hours showing potential vorticity (coloured) and potential temperature (contoured, interval 4 K) for (a) simulation NO-SBL, and (b) simulation NO-CBL.

Figure 5 shows cross-sections through the low centre for simulations NO-SBL and NO-CBL. As expected, simulation NO-SBL (Fig. 5a) has no PV anomaly present above the low centre. With no friction in the stable boundary-layer area, the surface stress is zero meaning that no PV generation by the baroclinic mechanism can occur there. There is no PV available to be ventilated on the warm-conveyor belt and a PV anomaly does not appear above the low centre. Hence for this simulation any spin-down effects must come from the Ekman pumping mechanism. There is still a peak of surface stress to the south and west of the low centre (not shown; similar to Figure 4b) and therefore an Ekman pumping velocity at the boundary-layer top above the low centre.

By comparison, simulation NO-CBL (Fig 5b) does show PV generation occurring near the cold front ($\approx$ 15E) and a PV anomaly located above the low centre. However, the generation does not appear as strong, nor the PV anomaly as well defined as in Figure 2a. Adamson *et al.* (2006) suggested that Ekman pumping in the region of the low centre helped to shape the PV anomaly in such a way that it was most associated with static stability, whilst enhancing the increased static stability by isentropic lifting within the boundary layer. This simulation, which lacks any Ekman pumping in the region of the low centre seems to support this view. The isentropes pass closer to the ground in the region of the low centre, demonstrating that they have not been lifted by the Ekman pumping. This leads to a PV anomaly which is weaker and less well-defined, with a lower static stability. Nevertheless, Figure 4a demonstrates that it is still capable of spinning down the cyclone, although not by as much as when the two mechanisms are combined.

Figure 4a also shows that the effects appear to add linearly, i.e. the sum of the spin-down created in simulations NO-SBL and NO-CBL appears to produce approximately the spin-down of the control simulation. However, the timing of the spin-down appears different between simulations NO-SBL and NO-CBL. Simulation NO-CBL appears to follow the evolu-

tion of simulation NO-BL, although with a reduced growth rate throughout the life-cycle. This is consistent with the baroclinic PV mechanism's effect on the tropospheric static stability. However, simulation NO-SBL appears to deepen rapidly (similar to NO-BL) at early times, but then to have a sharp reduction in growth rate after 50 hours. This is consistent with Ekman pumping becoming an important spin-down mechanism as the cyclone reaches occlusion and enters a barotropic decay phase. The control simulation then shows features of both, with a reduced growth rate throughout the simulation and a sharp reduction at ≈ 45 hours.

4 Conclusions

This paper has discussed two potential mechanisms by which the boundary layer can act to reduce the intensity of mid-latitude weather systems. Through a hierarchy of theoretical and computational models, it has been shown that the traditional Ekman pumping mechanism does not fully account for the internal dynamics of the boundary layer. It has often been assumed (e.g. Card and Barcilon, 1982; Farrell, 1985) that the boundary layer influence in baroclinic cyclones is governed entirely by the Ekman pumping process. However, the Eady model and more complicated numerical simulations have demonstrated that in a baroclinic cyclone, the three-dimensional structure and evolution of the boundary layer needs to be considered.

This highlights the importance of representing boundary-layer processes in the most realistic manner possible. Long-tailed stability functions have been shown to be unrealistic when compared to observations and large-eddy simulations (Beare *et al.*, 2006), but Beljaars and Viterbo (1998) discuss how they are required within numerical weather prediction (NWP) models to give the correct Ekman pumping within cyclones and improve NWP skill scores. The improvements they cause are likely to be a case of compensating errors, and recently Brown *et al.* (2008) have shown improved skill scores from the use of more realistic stability functions, combined with other improvements to the boundary-layer parametrization. This demonstrates that accurately representing all processes occurring within a cyclone boundary layer is important for accurate NWP, rather than tuning Ekman pumping to give the best simulation. Furthermore, the analysis presented here would seem to cast some doubt on the idea that the stability functions are actually tuning the Ekman pumping. We have shown that friction in the stable boundary-layer is associated more with the baroclinic PV mechanism, and so altering the stable boundary-layer parametrization may actually have been tuning the baroclinic PV mechanism.

Use of PV inversions demonstrated the shielding effect of a low-level PV anomaly formed by baroclinic frictional generation. The interaction between the mechanisms was established and investigated by modifying the boundary-layer characteristics. Selectively switching off the boundary-layer parametrization depending on stability attempted to separate the mechanisms, but instead demonstrated how the baroclinic PV mechanism is partly reliant on Ekman pumping in order to shape the low-level PV anomaly. Therefore, not only are both mechanisms

present in a single simulation (as concluded by Boutle *et al.*, 2007), but we have shown here that both mechanisms are of approximately equal importance and that they cannot be cleanly separated.

Acknowledgements

We would like to thank Bob Beare and Andy Brown for useful discussions of this work.

References

Adamson, D. S., Belcher, S. E., Hoskins, B. J., and Plant, R. S. (2006). Boundary-layer friction in midlatitude cyclones. *Q. J. R. Meteorol. Soc.*, **132**, 101–124.

Ahmadi-Givi, F., Craig, G. C., and Plant, R. S. (2004). The dynamics of a midlatitude cyclone with very strong latent-heat release. *Q. J. R. Meteorol. Soc.*, **130**, 295–323.

Anthes, R. A. and Keyser, D. (1979). Tests of a fine-mesh model over Europe and the United States. *Mon. Weather Rev.*, **107**, 963–984.

Beare, R. J. (2007). Boundary layer mechanisms in extratropical cyclones. *Q. J. R. Meteorol. Soc.*, **133**, 503–515.

Beare, R. J., MacVean, M. K., Holtslag, A. A. M., Cuxart, J., Esau, I., Golaz, J.-C., Jimenez, M. A., Khairoutdinov, M., Kosovic, B., Lewellen, D., Lund, T. S., Lundquist, J. K., McCabe, A., Moene, A. F., Noh, Y., Raasch, S., and Sullivan, P. (2006). An intercomparison of large-eddy simulations of the stable boundary layer. *Boundary-Layer Meteorol.*, **118**, 247–272.

Beljaars, A. C. M. and Viterbo, P. (1998). Role of the boundary layer in a numerical weather prediction model. In A. A. M. Holtslag and P. G. Duynkerke, editors, *Clear and Cloudy Boundary Layers*, pages 287–304, Royal Netherlands Academy of Arts and Sciences, Amsterdam.

Boutle, I. A. (2009). *Boundary-Layer Processes in Mid-latitude Cyclones*. Ph.D. thesis, University of Reading. http://www.met.rdg.ac.uk/phdtheses/Boundary Layer Processes in Mid-latitude Cyclones.pdf.

Boutle, I. A., Beare, R. J., Belcher, S. E., and Plant, R. S. (2007). A note on boundary-layer friction in baroclinic cyclones. *Q. J. R. Meteorol. Soc.*, **133**, 2137–2141.

Boutle, I. A., Beare, R. J., Belcher, S. E., Brown, A. R., and Plant, R. S. (2010). The moist boundary layer under a mid-latitude weather system. *Boundary-Layer Meteorol.*, **134**, 367–386.

Brown, A. R., Beare, R. J., Edwards, J. M., Lock, A. P., Keogh, S. J., Milton, S. F., and Walters, D. N. (2008). Upgrades to the boundary-layer scheme in the Met Office numerical weather prediction model. *Boundary-Layer Meteorol.*, **128**, 117–132.

Card, P. A. and Barcilon, A. (1982). The Charney stability problem with a lower Ekman layer. *J. Atmos. Sci.*, **39**, 2128–2137.

Davis, C. A. and Emanuel, K. A. (1991). Potential vorticity diagnostics of cyclogenesis. *Mon. Weather Rev.*, **119**, 1929–1953.

Eady, E. T. (1949). Long waves and cyclone waves. *Tellus*, **1**, 33–52.

Farrell, B. (1985). Transient growth of damped baroclinic waves. *J. Atmos. Sci.*, **42**, 2718–2727.

Pedlosky, J. (1979). *Geophysical Fluid Dynamics*. Springer, New York.

Plant, R. S. and Belcher, S. E. (2007). Numerical simulation of baroclinic waves with a parameterized boundary layer. *J. Atmos. Sci.*, **64**, 4383–4399.

Shapiro, M. A. and Keyser, D. (1990). Fronts, jet streams and the tropopause. In *Extratropical Cyclones: The Erik Palmén Memorial Volume*, pages 167–191. Amer. Meteorol. Soc., Boston.

Sinclair, V. A., Belcher, S. E., and Gray, S. L. (2010). Synoptic controls on boundary-layer characteristics. *Boundary-Layer Meteorol.*, **134**, 387–409.

Stoelinga, M. T. (1996). A potential vorticity-based study of the role of diabatic heating and friction in a numerically simulated baroclinic cyclone. *Mon. Weather Rev.*, **124**, 849–874.

Valdes, P. J. and Hoskins, B. J. (1988). Baroclinic Instability of the Zonally Averaged Flow with Boundary Layer Damping. *J. Atmos. Sci.*, **45**, 1584–1593.

Ziemianski, M. (1994). Potential vorticity inversion. *Joint Centre for Mesoscale Meterology (JCMM) Internal Report*, **39**. University of Reading, Reading, UK.